Hydroxyapatite nanopowders prepared in the presence of zirconium ions

M. J. Lukić*[1], Lj. Veselinović[1], M. Stevanović[1], J. Nunić[2], G. Dražič,[3] S. Marković[1], D. Uskoković[1]

[1]Institute of Technical Sciences of the Serbian Academy of Sciences and Arts, Belgrade, Serbia

[2]Department of Genetic Toxicology and Cancer Biology, National Institute of Biology, Ljubljana, Slovenia

[3]Laboratory for Materials Chemistry, National Institute of Chemistry, Ljubljana, Slovenia

*corresponding author: miodrag.lukic@itn.sanu.ac.rs

Abstract

Hydroxyapatite nanopowders were prepared in the presence of different concentrations of zirconium ions. Such crystallization conditions yielded significantly reduced particle size and increased specific surface area. Cell viability and oxidative stress studies showed that biocompatibility was not impaired when compared to pure hydroxyapatite. Non-isothermal sintering implied the possibility for suppressing the reaction between hydroxyapatite and zirconia by limiting it to only calcium phosphates. Stress-induced transformation of tetragonal to monoclinic is facilitated by total hydroxyapatite to β-tricalcium phosphate phase transformation.

Keywords: biomaterials, bioceramics, FTIR, sintering

Introduction

The improvement of material properties without negatively affecting the biological response is a permanently targeted issue concerning bioceramics. Hydroxyapatite (HAp) is a bioactive material

and one of the most suitable ceramics for bone and dental tissue reconstruction, but still lacks adequate mechanical properties. However, zirconia (ZrO_2) offers good mechanical response, but has a disadvantage of poor bonding to host tissue. Their composites are quite promising, though, offering many potential biological and structural advantages. HAp/ZrO_2 composites are usually prepared by physical mixing or colloidal dispersions of ZrO_2 with HAp [1]. The addition of other phases to HAp influences its bioactivity and phase stability during sintering [2]. Procedures that reduce the amount of reinforcing agents have already been investigated [3]. Also, pressureless densification of HAp/ZrO_2 is difficult because of the mismatch in thermal expansion coefficients and requires field-assisted sintering techniques and tetragonal ZrO_2 (t-ZrO_2) stabilization since there is a tendency to reactions between HAp and ZrO_2 [4,5].

In this study, the preparation of HAp nanopowders in the presence of different amounts of zirconium ions was performed under reflux conditions. Detailed structural and chemical characterizations were performed, while biocompatibility was determined in cytotoxicity and oxidative stress studies. Non-isothermal sintering was performed up to 1300 °C and the results were correlated with the phase composition.

Materials and methods

Chemical precipitation has been performed with following precursors: calcium nitrate tetrahydrate, $Ca(NO_3)_2 \cdot 4H_2O$, (Fluka Analytical, Germany), zyrconyl chloride octahydrate, $ZrOCl_2 \cdot 8H_2O$, (The British Drug Houses Ltd., United Kingdom) and ammonium dihydrogen phosphate, $NH_4H_2PO_4$, (Zorka Šabac, Serbia). Concentrations were adjusted to retain (Ca+Zr)/P molar ratio of 1.67 for different amounts of zirconium (0, 1, 5 and 10 at.% with respect to Ca), denoted as HAp-X (X= 0, 1, 5, 10), respectively. Reactants were dissolved in 80 ml of distilled water each and heated to 70 °C. The solutions of calcium and zirconium ions were mixed, followed by the addition of a phosphate solution and precipitation by the dropwise addition of 10 ml of NH_4OH to reach pH 11. The reaction batch (250 ml), enclosed in reflux conditions to

provide constant pH in the presence of small amount of NH_4OH, was effectively stirred for 3 h at 70 °C, with afterward ageing, washing out to pH 7 and drying. The phase analysis was carried out using X-ray diffraction (Philips PW-1050). The FTIR measurement was performed in the spectral range of 400–4000 cm^{-1} (BOMEM, Hartmann& Braun). Particle size and morphology were investigated using transmission electron microscopy (TEM, JEOL 2100); elemental mapping was performed by EDXS analysis (JEOL ARM 200 CF equipped with JEOL centurion 100). The specific surface area (SSA) was measured by Brunauer–Emmett–Teller (BET) technique with N_2 adsorption–desorption isotherms at −195.8 °C (Micromeritics Gemini 2370 V5).

For determination of the biological response we used HepG2 cells, which were obtained from the European Collection of Cell Cultures (UK) and were grown as described previously [6]. The cytotoxicity was determined with 3-(4,5-dimethylthiazol-2-yl)-2,5-diphenyltetrazolium bromide (MTT) according to Mosmann [7], with minor modifications [6]. The HepG2 cells were seeded onto 96-well microplates (Nunc, Naperville IL, USA) at a density of 40000 cells/ml and incubated for 20 h at 37 ^{o}C to attach. The medium was replaced by fresh medium containing 0, 0.00001, 0.0001, 0.001, 0.01 and 0.1 % (w/v) of HAp-X (X = 0, 1, 5, 10) samples and incubated for 24 h. In each experiment a negative control (non-treated cells) was included. The protocol was continued as described previously [6]. Cell survival was determined by comparing the optical density of the wells containing the treated cells with those of the negative control.

The formation of intracellular reactive oxygen species (ROS) was measured spectrophotometrically using the fluorescent probe DCFH-DA [8], with minor modifications [6]. The HepG2 cells were seeded at a density of 75000 cells/ml into 96-well, black microplates (Nunc, Naperville IL, USA) in five replicates and incubated for 20 h at 37 °C to attach. After that, the cells were incubated with 20 mM DCFH-DA for 30 min, then DCFH-DA was removed, and cells were washed out with PBS and treated with concentrations 0, 0.00001, 0.0001, 0.001, 0.01 and 0.1 % (v/v) of HAp-X (X= 0, 1, 5, 10) samples. Negative control (non-treated cells) and

positive control (0.5 mM tert-butyl hydroperoxide treated) were always included. The protocol was continued as described previously [6].

The powders were uniaxially pressed under 100 MPa. Non-isothermal sintering was performed to 1300 °C in a heating microscope (New Heating Microscope EM201, Hesse Instruments) with the heating rate of 10 °C/min.

Results and discussion

XRD patterns of the prepared materials, Fig. 1a, showed the reflections characteristic for HAp. The only difference among these samples was the diffuse scattering in 20-40^{o} *2θ* range for HAp-10 sample, which could originate from ZrO_2 phase [9].

FTIR spectra, Fig. 1b, of the synthesized powders were almost identical, showing typical apatite phosphate (PO_4^{3-}) modes at: 470 cm^{-1} (ν2 bending vibration), 564 and 602 cm^{-1} (ν4 bending vibration), 962 cm^{-1} (ν1 symmetric stretching vibration), and in the 1000–1150 cm^{-1} region (ν3 asymmetric stretching mode). The bands at 1637 and in the 3000–3650 cm^{-1} range are attributed to associated water. The O–H libration and stretching modes appeared at 632 and 3570 cm^{-1}, respectively. Vibrational bands at 669, 875 cm^{-1} and in the 1450–1500 cm^{-1} region are attributed to ν4, ν2 and ν3 stretching modes of incorporated carbonates, respectively.

Deconvolution of 400–750 cm^{-1} spectral region of HAp-5 and HAp-10 yielded three more peaks centered at 425, 525, and 580 cm^{-1} that could be attributed to Zr–O stretching mode [10], suggesting the formation of ZrO_2 phase and the existence of HAp/ZrO_2 composite.

The results of TEM analysis, shown in Fig. 2, revealed that all the prepared powders possessed uniform particles. However, with higher concentrations, both the particle size and their aspect ratio changed. The particles of HAp-0 were 150 nm long and around 20 nm wide, while those of HAp-10 had the length of around 45 nm and the width of less than 10 nm, with more rounded morphology. The EDXS analysis showed that ZrO_2 is uniformly dispersed within the

samples; slight aggregation was observed for higher initial concentrations of zirconium. The size of zirconia particulates is around 25 nm, with rounded morphology. Reduction of the particle size led to an increase of SSA, being 74, 73, 126, and 137 m^2/g for HAp-X (X= 0, 1, 5, 10) samples, respectively.

Biocompatibility studies of the prepared nanopowders confirmed that the initial properties of pure HAp were not impaired with the addition of zirconium ions. The cytotoxicity determined by MTT assay after 24 h exposure, Fig. 3a, revealed that all samples have concentration-dependent, but comparable levels of cytotoxicity, independent on the amount of zirconium ions. On the other side, measurements of the oxidative stress induced in Hep G2 cells, Fig. 3b, showed that all the samples after 5 h induced favourable response, without significant generation of ROS. Only the highest concentration showed the ROS increase.

From non-isothermal sintering studies, Fig. 4a, very different sintering behavior was found and correlated to the phase composition, Fig. 4b. HAp-0 sample sintered around 1100 °C remained pure HAp phase due to stoichiometric Ca/P ratio. HAp-1 sample had a lower bulk density and the dominant presence of HAp phase with a small amount of β-tricalcium phosphate (β-TCP) phase and the appearance of t-ZrO_2. The lower density is explained by densification suppression in the presence of TCP phases with lower theoretical densities (2.86, 3.07 and 3.16 gcm^{-3} for α-TCP, β-TCP and HAp, respectively). HAp-5 showed better densification comparing to HAp-1. Phase composition analysis revealed a higher amount of t-ZrO_2 phase in co-existence with HAp and α-TCP»β-TCP phases. The fact that HAp-1 and HAp-5 retained t-ZrO_2 could be suitable for formation of BCP/ZrO_2 [11]. The formation of cubic zirconia and/or calcium zirconate above 1200 °C [12], which could inhibit the toughening mechanism through transformation of t-ZrO_2 to m-ZrO_2, was not observed. Since HAp-1 and HAp-5 are basically Ca-deficient HAp, they decompose above 700 °C and prevent the reaction between HAp and t-ZrO_2.

HAp-10 sample showed two distinct sintering regions: enhanced sintering up to 900 °C and subsequent retardation from 900 to 1100 °C. Biodegradable β-TCP appeared as the only

calcium phosphate phase, while m-ZrO_2 was the dominant phase compared to t-ZrO_2. The explanation for such a phase composition is related to the initial Ca/P ratio of HAp-10 sample, being 1.5, which yields total decomposition of HAp to β-TCP; that is accompanied with sudden volume expansion, which could provoke stress-induced transformation of t-ZrO_2 to m-ZrO_2. This is expressed as retardation in the sintering curves, Fig. 4a. It is important to observe that HAp-10 starts sintering at 800 °C due to Ca^{2+} vacancies in HAp crystal lattice. As a suggestion for the further research, phase transformation stresses could be avoided in water vapor atmosphere, and the final system could retain t-ZrO_2, susceptible to transformation toughening under mechanical loading.

Conclusions

Hydroxyapatite nanopowders were successfully prepared in the presence of zirconium ions. With zirconium addition, the particle morphology became more rounded and the particle size significantly decreased, from 150 to 45 nm in length and from 20 to 10 nm in width, yielding the doubling of SSA. Biocompatibility was not altered compared to pure HAp. Sintering studies showed that the phase composition could be tailored by the appropriate choice of zirconium amount and that HAp-1 and HAp-5 samples exhibited the presence of only t-ZrO_2 after non-isothermal sintering. For HAp-10 sample, it was shown that the complete phase transformation from HAp to β-TCP provoked stress-induced transformation of t-ZrO_2 to m-ZrO_2. Using HAp with Ca/P ratio $1.67 \leq x \leq 1.5$, the reaction between HAp and ZrO_2 is suppressed by providing an alternative, less energy-consuming pathway of Ca-deficient HAp decomposition, confining the reaction only to the calcium phosphate phase.

Acknowledgements

This study was supported by the Ministry of Education, Science and Technological Development of the Republic of Serbia under grant no. III45004. The authors are thankful to Dr. Ines Bračko for TEM measurements.

References

[1] Sung Y-M, Shin Y-K, Ryu J-J. Preparation of hydroxyapatite/zirconia bioceramic nanocomposites for orthopaedic and dental prosthesis applications. Nanotechnology 2007;18:065602.

[2] Sultana R, Yang J, Hu X. Deposition of micro-porous hydroxyapatite/tri-calcium phosphate coating on zirconia-based substrate. J Am Ceram Soc 2012;95:1212–5.

[3] Ahn ES, Gleason NJ, Ying JY. The Effect of zirconia reinforcing agents on the microstructure and mechanical properties of hydroxyapatite-based nanocomposites J Am Ceram Soc 2005;88:3374–9.

[4] Ergun C. Enhanced phase stability in hydroxylapatite/zirconia composites with hot isostatic pressing. Ceram Int 2011;37:935-42.

[5] Gergely G, Sahin FC, Göller G, Yücel O, Balázsi C. Microstructural and mechanical investigation of hydroxyapatite–zirconia nanocomposites prepared by spark plasma sintering. J Eur Ceram Soc 2013;33:2313-19.

[6] Petković J, Žegura B, Stevanović M, Drnovšek N, Uskoković D, Novak S, Filipič M. DNA damage and alterations in expression of DNA damage responsive genes induced by TiO_2 nanoparticles in human hepatoma HepG2 cells. Nanotoxicology 2011;5:341–53.

[7] Mosmann T. Rapid colorimetric assay for cellular growth and survival: Application to proliferation and cytotoxicity assays. J Immunol Methods 1983;65:55–63.

[8] Osseni R, Debbasch C, Christen M-O, Rat P, Warnet J-M. Tacrine-induced Reactive Oxygen Species in a Human Liver Cell Line: The Role of Anethole Dithiolethione as a Scavenger. Toxicol In Vitro 1999;13:683–8.

[9] Chaudhry AA, Yan H, Viola G, Reece MJ, Knowles JC, Gong K, Rehman I, Darr JA. Phase stability and rapid consolidation of hydroxyapatite–zirconia nano-coprecipitates made using continuous hydrothermal flow synthesis. J Biomater Appl 2012;27:79–90.

[10] Manivasakan P, Rajendran V, Rauta PR, Sahu BB, Panda BK. Synthesis of monoclinic and cubic ZrO_2 nanoparticles from zircon. J Am Ceram Soc 2011;94:1410–20.

[11] Kim M, Franco RA, Lee B-T. Synthesis of functional gradient BCP/ZrO_2 bone substitutes using ZrO_2 and BCP nanopowders. J Eur Ceram Soc 2011;31:1541-8.

[12] Evis Z, Usta M, Kutbay I. Improvement in sinterability and phase stability of hydroxyapatite and partially stabilized zirconia composites. J Eur Ceram Soc 2009;29:621-8.

Figure captions

Fig. 1 a) XRD patterns and b) FTIR spectra of precipitated powders.

Fig. 2 TEM micrographs of prepared nanopowders; EDXS mapping of Zr density, and Ca and Zr concentration.

Fig. 3 a) MTT assay and b) ROS study of prepared nanopowders.

Fig. 4 a) Non-isothermal sintering curves to 1300 °C and b) corresponding XRD patterns.

Fig. 1.

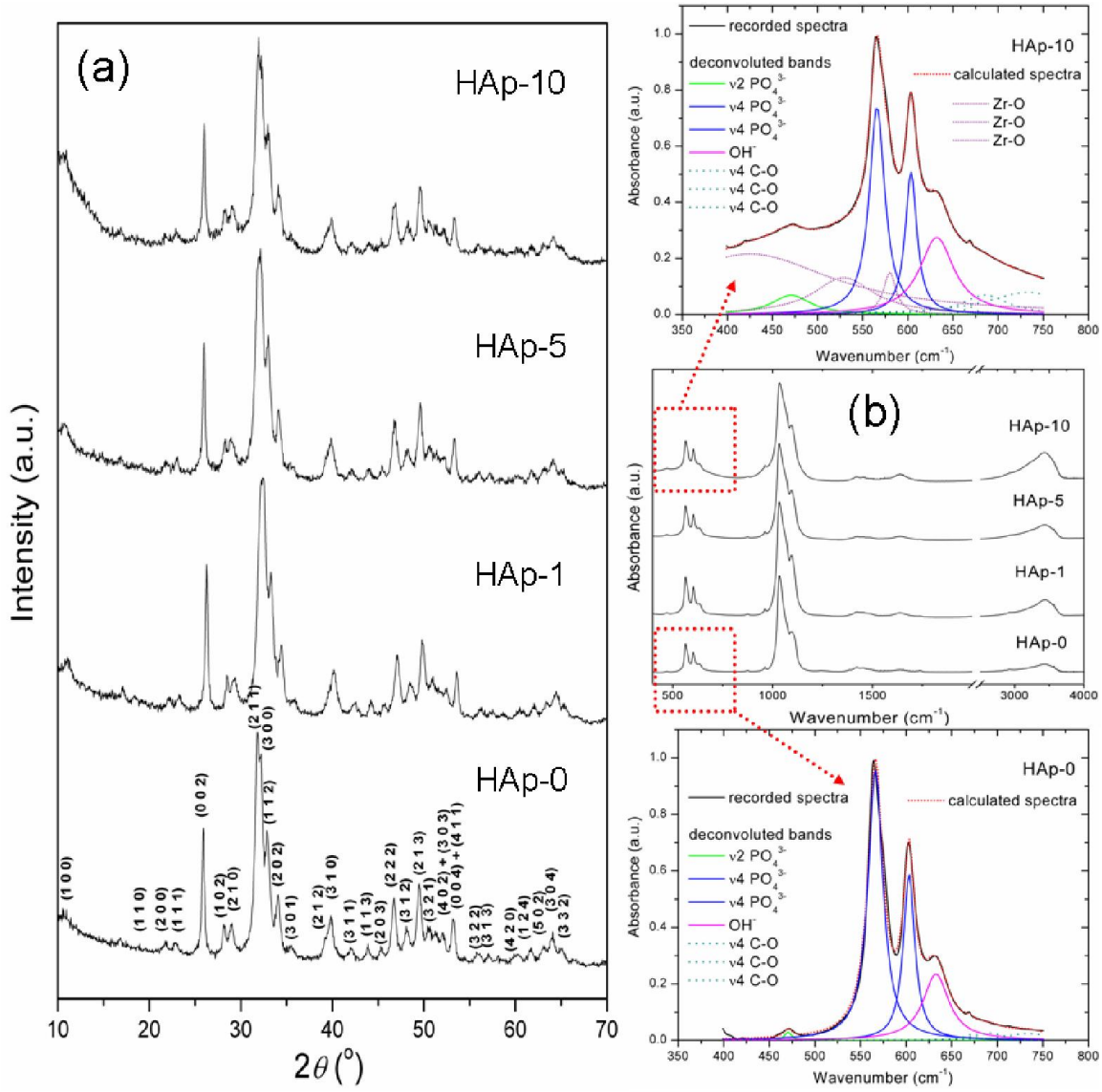
(a)
HAp-10
HAp-5
HAp-1
HAp-0
Intensity (a.u.)
2θ (°)
(b)
recorded spectra
deconvoluted bands
calculated spectra
Zr-O
Absorbance (a.u.)
Wavenumber (cm-1)

Fig. 2.

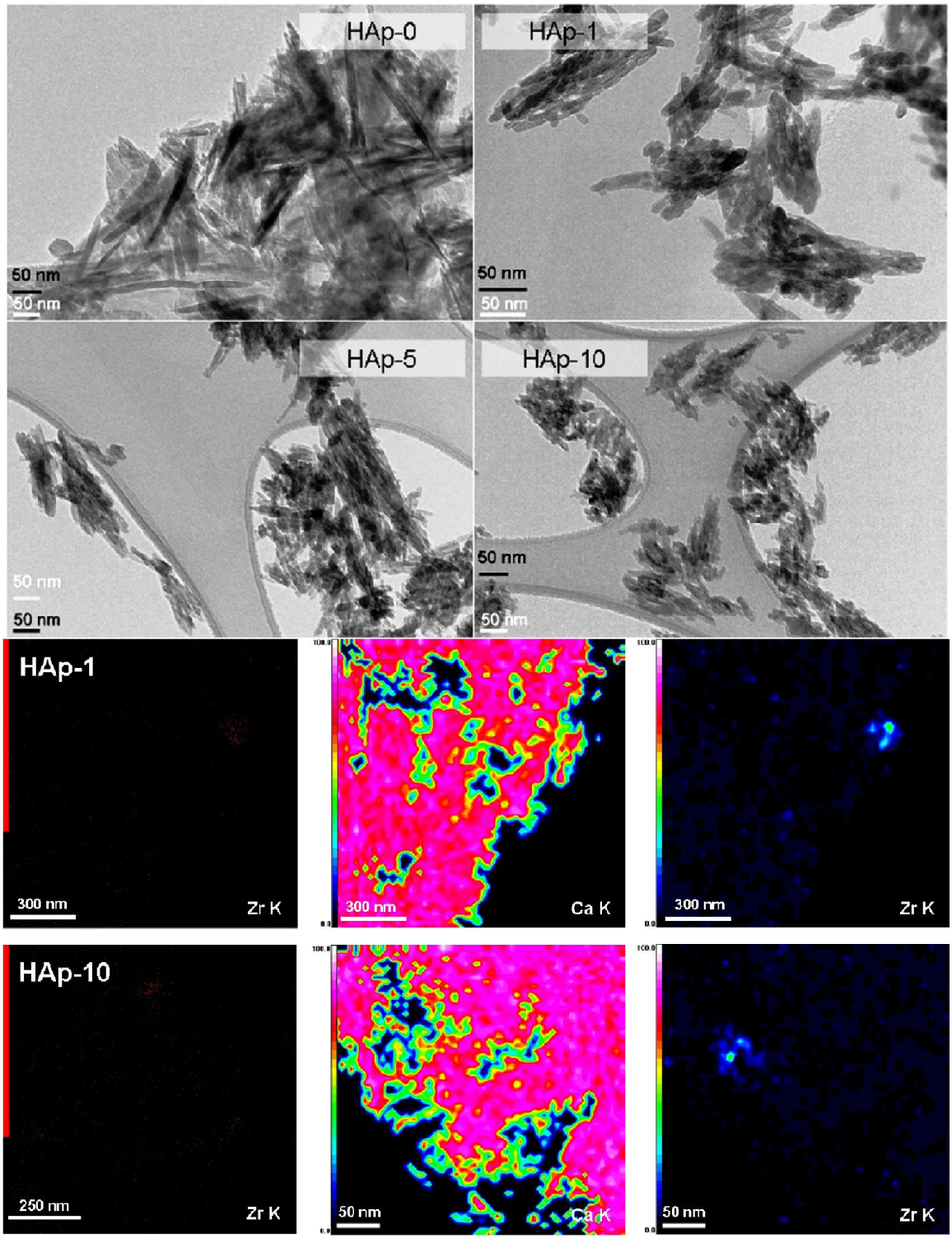
HAp-0
50 nm
HAp-1
50 nm
HAp-5
50 nm
HAp-10
50 nm
HAp-1
300 nm
Zr K
300 nm
Ca K
300 nm
Zr K
HAp-10
250 nm
Zr K
50 nm
Ca K
50 nm
Zr K

Fig. 3.

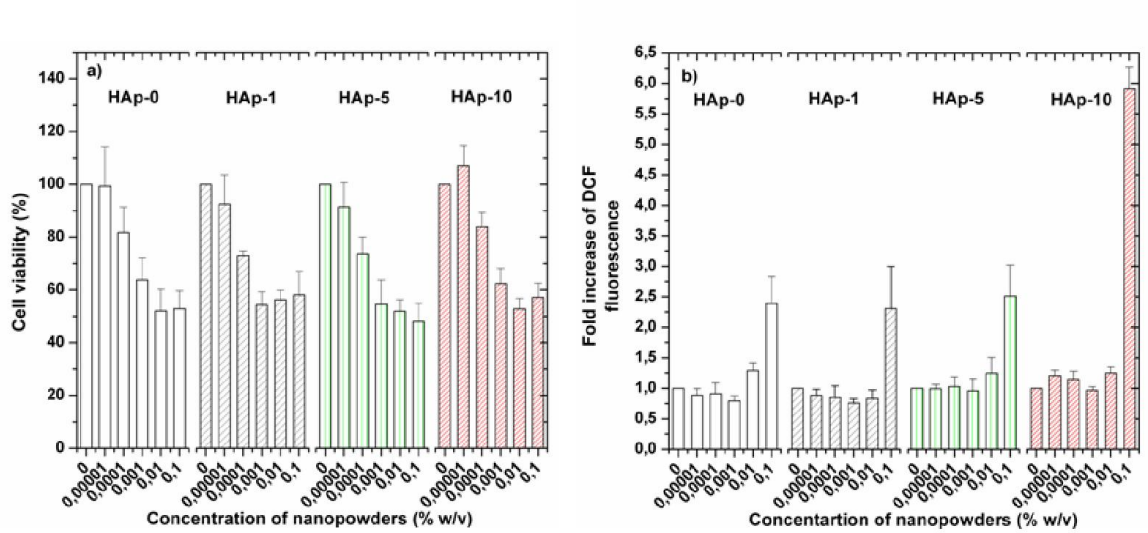
a)
HAp-0
HAp-1
HAp-5
HAp-10
Cell viability (%)
Concentration of nanopowders (% w/v)
b)
HAp-0
HAp-1
HAp-5
HAp-10
Fold increase of DCF fluorescence
Concentartion of nanopowders (% w/v)

Fig. 4.

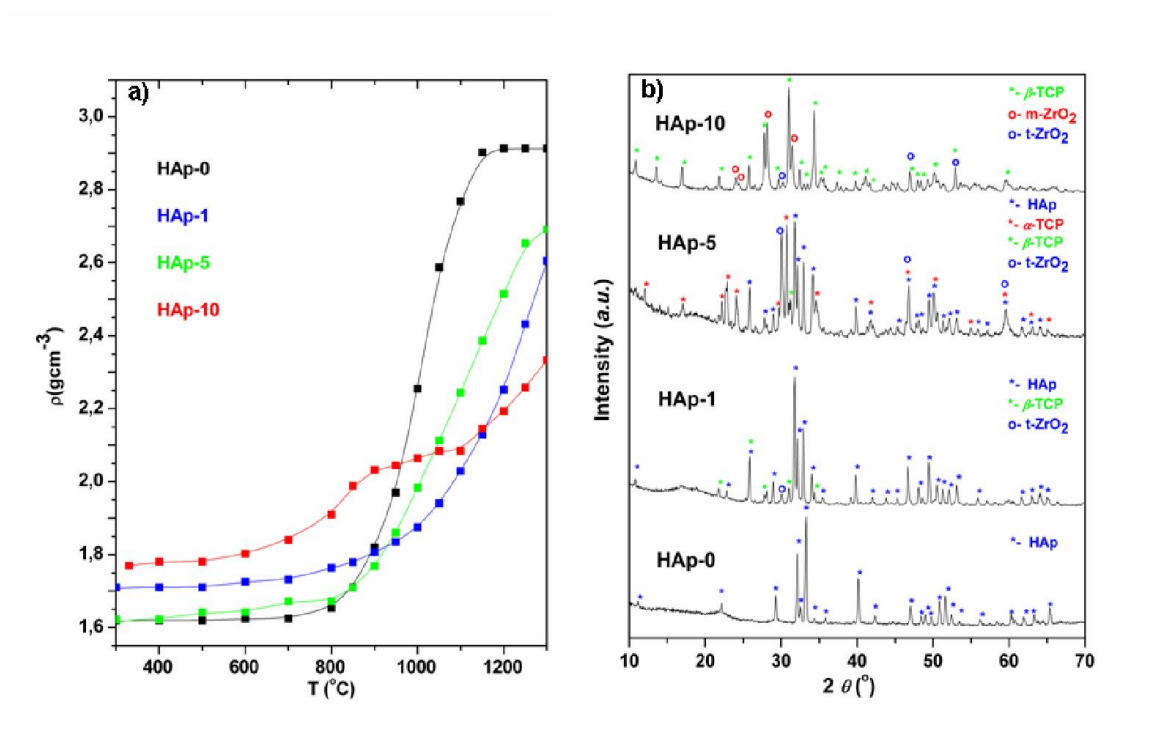
a)
HAp-0
HAp-1
HAp-5
HAp-10
ρ(gcm-3)
T (°C)
b)
HAp-10
*- β-TCP
o- m-ZrO2
o- t-ZrO2
HAp-5
*- HAp
*- α-TCP
*- β-TCP
o- t-ZrO2
HAp-1
*- HAp
*- β-TCP
o- t-ZrO2
HAp-0
*- HAp
Intensity (a.u.)
2 θ (°)